Received: 30 October 2019 | Revised: 15 January 2020 | Accepted: 16 January 2020

DOI: 10.1002/pro.3829

THE PROTEIN SOCIETY WILEY

ARTICLE

Conformational states of TNFR1 as a molecular switch for receptor function

Chih Hung Lo | **Evan C. Huber** | **Jonathan N. Sachs**

Department of Biomedical Engineering, University of Minnesota, Minneapolis, Minnesota

Correspondence
Jonathan N. Sachs, Department of Biomedical Engineering, 7-126 Nils Hasselmo Hall, 312 Church St. SE, Minneapolis, MN 55455.
Email: jnsachs@umn.edu

Funding information
National Institutes of Health, Grant/Award Numbers: R01GM107175, R35GM131814; University of Minnesota, Grant/Award Number: Doctoral Dissertation Fellowship; Office of Research Infrastructure Programs, Grant/Award Number: 1S10OD021539-01

Abstract

Tumor necrosis factor receptor 1 (TNFR1) is a transmembrane receptor that plays a key role in the regulation of the inflammatory pathway. While inhibition of TNFR1 has been the focus of many studies for the treatment of autoimmune diseases such as rheumatoid arthritis, activation of the receptor is important for the treatment of immunodeficiency diseases such as HIV and neurodegenerative diseases such as Alzheimer's disease where a boost in immune signaling is required. In addition, activation of other TNF receptors such as death receptor 5 or FAS receptor is important for cancer therapy. Here, we used a previously established TNFR1 fluorescence resonance energy transfer (FRET) biosensor together with a fluorescence lifetime technology as a high-throughput screening platform to identify a novel small molecule that activates TNFR1 by increasing inter-monomeric spacing in a ligand-independent manner. This shows that the conformational rearrangement of pre-ligand assembled receptor dimers can determine the activity of the receptor. By probing the interaction between the receptor and its downstream signaling molecule (TRADD) our findings support a new model of TNFR1 activation in which varying conformational states of the receptor act as a molecular switch in determining receptor function.

KEYWORDS

conformational states, FRET, high-throughput screening, small molecule activator, structural dynamics, TNFR1 signaling

1 | INTRODUCTION

The receptors and ligands in the tumor necrosis factor (TNF) superfamily have unique structural attributes that couple them directly to signaling pathways that are responsible for a wide range of cellular activities such as cell proliferation, differentiation, or death.[1,2] Within this superfamily, tumor necrosis factor receptor 1 (TNFR1) is a characteristic member and a central mediator in the signal transduction of the inflammatory pathway.[3] Stimulation by the native ligands of TNFR1, tumor necrosis factor-alpha (TNFα) and lymphotoxin-alpha (LTα), leads to the recruitment of TNFR1 associated death domain (TRADD) followed by IκBα degradation and NF-κB activation.[4] While over-activation of TNFR1 results in excessive NF-κB activation, which has been associated with several autoimmune diseases such as rheumatoid arthritis,[3–5] lack of NF-κB activation has been implicated in diseases related to immune deficiency and cell death such as HIV, neurodegeneration, and tissue degeneration.[6–9] Hence, there is a need for increased activation of TNFR1 beyond its native activation to promote NF-κB activation for treatment of these diseases.[10–15] In addition, activation of other TNF receptors such as death receptor 5 (DR5) or FAS receptor is important for cancer therapy.[16–19]

Current methods of TNFR1 activation include ligand mimics such as *Staphylococcus aureus* protein A, which has been shown to act as a ligand and mimic TNFα in order to activate TNFR1.[20] Burkholderia cenocepacia BC7 also has been shown to bind to and activate TNFR1.[21] Another way to increase the activation of TNFR1 is by increasing the expression of TNFR1 in cells,[22] though the presence of native ligand is still required for the receptor activation. The limitation for proteins that mimic the ligand is that they compete with native ligand binding, diminishing the potential elevated effects in activating TNFR1. Hence, the most effective way to activate TNFR1 would be a receptor-specific approach that activates the receptor regardless of ligand stimulation or amplifies the effect of ligand stimulation by making use of the receptor structure and conformational states.

Recent evidence has revised the long-held view of TNFR activation as structurally rigid monomers, instead showing that the preassembled receptor dimer remains intact upon ligand binding, potentially forming the nexus for larger-scale networks of conformationally active ligand-bound TNFR trimers.[23–26] This model reconciles the seeming inconsistency between the two crystal structures of TNFR1: (a) trimerization induced by ligand binding without direct receptor–receptor interactions;[27] and (b) TNFR1 forms pre-ligand assembled dimers held together by the pre-ligand assembly domain (PLAD).[28–30] Several efforts have directly targeted the receptor dimer to alter its function based on this revised model. In our previous work, we have shown that disruption of receptor–receptor interactions by zafirlukast, a small molecule, without ablating ligand binding inhibits TNFR1 signaling, supporting the oligomeric network model.[31] In addition, we have also shown that small molecule allosteric inhibitors (e.g., DS42) exert their inhibitory effect by altering the conformational state of the preassembled dimer without blocking ligand binding or dimerization, demonstrating that TNFR1 can be inactive, even if ligand is bound and the receptor dimer is intact.[32] This suggests the possibility that, in contrast to receptor inhibition, enhanced TNFR1 activity (relative to native levels) could be achieved through stabilizing active conformations. This possibility is supported by a study showing that ligand binding causes a conformational change in the preassembled TNFR1 complex as measured by fluorescence resonance energy transfer (FRET), though the exact activation mechanism was not delineated.[33,34] In addition, we used FRET to show that a disease-related mutant (R92Q), which is constitutively active, also forms a pre-ligand assembled dimer.[35] Importantly, our FRET measurements showed that this active R92Q dimer is conformationally distinct from wild-type, suggesting the correlation between the TNFR1 conformational states and receptor activity. Furthermore, our recent computational and experimental results suggest that long-range perturbation of TNFR1 conformational dynamics mediated by the ligand-binding loop with signal propagation through the backbone of the extracellular domain (ECD) is a feasible approach to control receptor function.[32,35] Besides TNFR1, we have previously shown that DR5, another receptor in the TNF superfamily, forms pre-ligand dimers that adopts an open and active conformational state upon binding of ligands.[36–39] In addition, other groups have reported the conformational dynamics of TNF receptors (e.g., TNFR2, RANK, FAS, TLR, and NTR[26,40–43]) and membrane receptors in general (e.g., EGFR and FGFR[44–46]).

The goal of this study was to determine whether small molecules could be used to force TNFR1 into an active conformational state that enhances signal propagation, which would be distinctly different from the small molecule inhibitors of TNFR1 previously discovered by our group.[31,32] To do this, we used the previously established TNFR1 FRET biosensor[31] in conjunction with a fluorescence lifetime detection technology[47,48] to perform high-throughput screening (HTS) on the library of pharmacologically active compounds (LOPAC) to discover small molecules that perturb the pre-ligand assembled TNFR1 dimer. We discovered a small molecule, SB 200646 hydrochloride (SBH), which binds TNFR1, reduces FRET of the biosensor and importantly, increases NF-κB activation by the same fold change in both the presence and absence of the ligand. As a control, we show that the activating effect of SBH is diminished in TNFR1 knockout cells, suggesting that the compound requires TNFR1 to activate the NF-κB pathway. Furthermore, we show that SBH exerts its effect through a conformationally active region of the receptor that we have previously identified.[32] Probing the interaction between the receptor and its downstream signaling molecule, we illustrated that the open conformation of TNFR1 allows its death domain to be more accessible to the recruitment and binding of TRADD, contributing to the enhanced receptor activation. Hence, we suggest that the ensemble of TNFR1 conformational states can be biased by small molecules toward those states associated with activation, hence acting like a molecular switch.

2 | RESULTS

2.1 | SBH perturbs the structural dynamics of pre-ligand assembled TNFR1 dimer to adopt an open conformation

To identify small molecules that modulate TNFR1 conformational states, we performed HTS of the LOPAC containing 1,280 compounds using our previously established

stable cell lines expressing a TNFR1 FRET biosensor (TNFR1ΔCD-FRET pair construct).[31,32] The TNFR1 FRET biosensor was engineered by fusing a green or red fluorescent protein (GFP or RFP) to the C-terminus of TNFR1 with a truncated cytosolic domain (ΔCD) (TNFR1ΔCD-GFP as donor and TNFR1ΔCD-RFP as acceptor) and was expressed in living HEK293 cells (Figure 1a). The FRET biosensor was validated for its capability to detect changes in cytosolic spacing between the pre-ligand receptor monomers in response to a change in the backbone conformation of the receptor induced by noncompetitive small molecule functional effectors[31,32] (Figure 1a). The coupling between fluorescent biosensor engineering and a high-throughput fluorescence lifetime plate-reader technology allows for increased precision and sensitivity as well as reliable detection of subtle changes in protein structures or conformational states induced by allosteric small molecule effectors.[49]

The FRET efficiency for all of the compounds, after removing the fluorescence interfering compounds, was plotted (Figure 1b) and the distribution of efficiency was fitted to a Gaussian distribution to obtain a mean and *SD* (Figure 1c). We also performed a donor-only screen as a control to further remove compounds that affect the fluorophores rather than the receptor. We found three compounds that showed up as hits in both donor-only screen and FRET screen, which were removed as false positives (Figure S1A,B, highlighted in pentagons]. After removing the false positives, there were only three reproducible hits that altered FRET by more than the 4*SD* threshold that we set for hit selection and all of them happen to decrease FRET of the biosensor (Figure 1b,

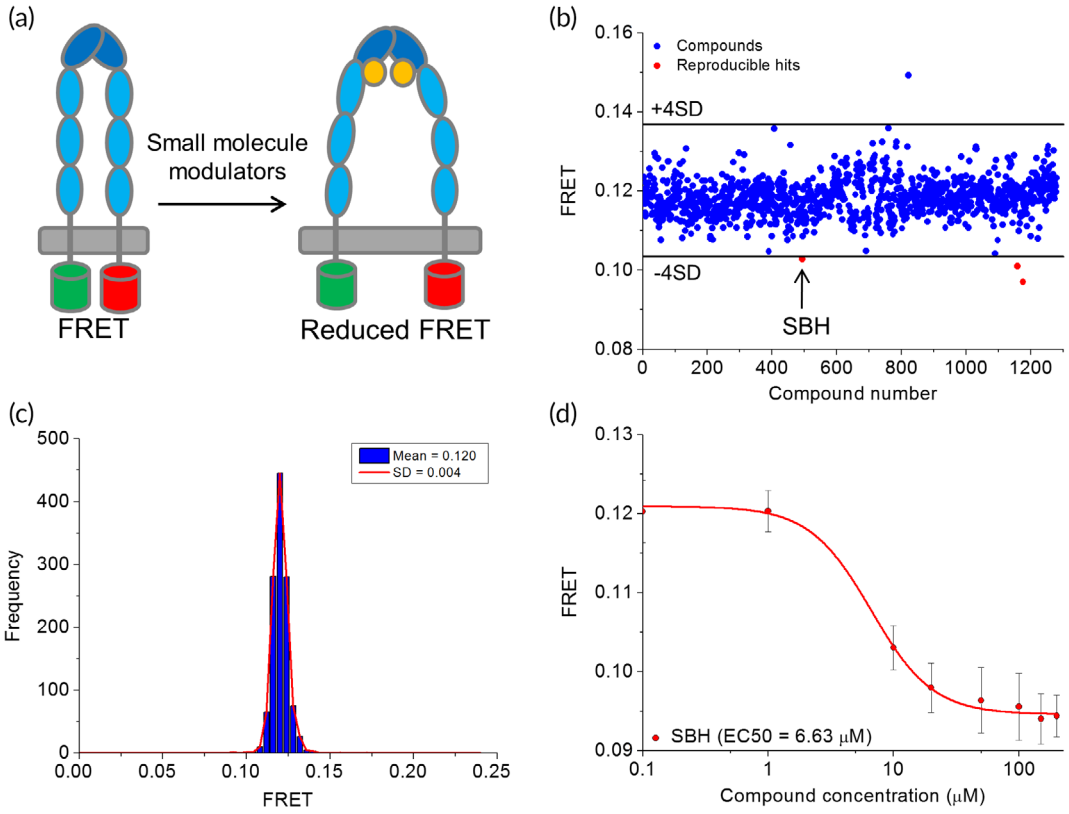

FIGURE 1 Small molecules probe conformational states of pre-ligand assembled TNFR1 dimer. (a) Schematic of the TNFR1ΔCD-FRET biosensor engineered by fusing the green or red fluorescent proteins (GFP or RFP) to the C-terminus of TNFR1 with truncated cytosolic domain. Ligand-independent association of the fluorophore-tagged receptors through PLAD-PLAD interactions results in fluorescence resonance energy transfer (FRET). The FRET biosensor is capable of detecting changes in the cytosolic spacing between receptor monomers. Small molecules targeting the receptor will induce a FRET change in the biosensor. (b) High-throughput screening of a library of pharmaceutically active compounds (LOPAC) using the TNFR1 FRET biosensor expressed in HEK293 cells. Potential false positives were removed from the screening plot and reproducible hits were selected based on a 4 standard deviations (4*SD*) threshold (black line). A novel activator of TNFR1 signaling, SB 200646 hydrochloride (SBH), was identified among the reproducible hits (arrow). Data are representative of three independent experiments. (c) Histogram plot of all compounds from the LOPAC screen after removal of false positives to obtain the average FRET efficiency and the *SD* of the screen. (d) Secondary FRET analysis of the dose-response of SBH. Data are means ± *SD* from three independent experiments

highlighted in red), indicating an opening in the inter-monomeric receptor spacing. As will be shown below, SBH (indicated by the arrow) was the only activator. SBH was then tested in a dose-response FRET assay and it showed a dose-dependent decrease in FRET efficiency with a half-maximal effective concentration (relative EC_{50}) of 6.6 μM (Figure 1d), confirming its direct interaction with the biosensor.

2.2 | SBH is a small molecule activator that stimulates TNFR1-induced NF-κB signaling pathway in the absence of ligand

The functional effect of SBH in the absence of ligand was first determined by monitoring IκBα degradation using immunoblotting in human embryonic kidney 293 cells (HEK293) with ligand-only treatment as a positive control (Figure 2a). Cells treated with SBH (200 μM) in the absence of ligand showed a significant degradation of IκBα to around half the basal amount in the control cells, indicating a twofold increase in the activation of the TNFR1 signaling pathway (Figure 2b). However, the amount of IκBα degraded with treatment of SBH was less than that degraded upon LTα treatment as a positive control, which was sixfold less than the basal level (Figure 2b). We then tested the effect of SBH in NF-κB activation in HEK293 cells in the absence of ligand using a luciferase assay. As a positive control, we treated cells with ligand only and observed a sixfold increase in the luciferase activity (Figure 2c), consistent with the observation from IκBα degradation assay. Cells treated with SBH in the absence of ligand showed a dose-dependent increase in NF-κB activation to twofold the basal activity with a relative EC_{50} value of 6.8 μM (Figure 2d). We note that the activating effect of SBH in both IκBα degradation and NF-κB activation assays

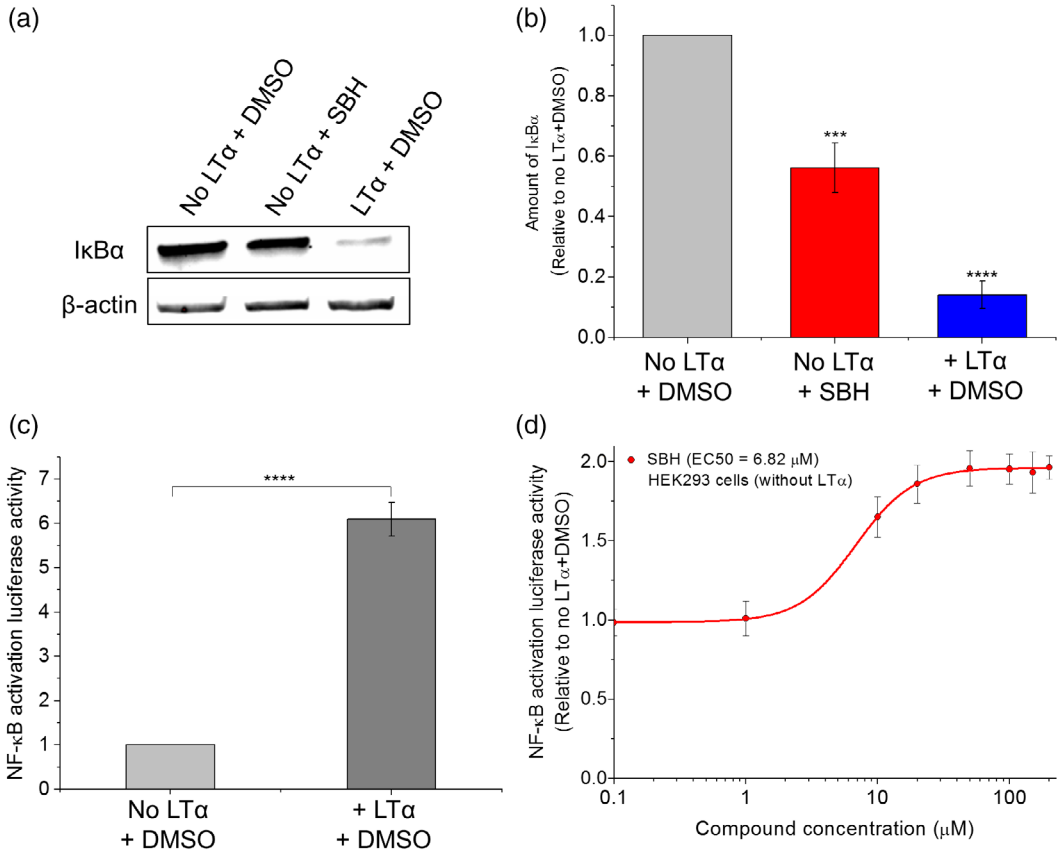

FIGURE 2 Effect of small molecule activator (SBH) on TNFR1-stimulated signaling in the absence of ligand. (a) Western blot analysis of the amount of IκBα in lysates of HEK293 cells treated with (1) no ligand and DMSO, (2) no ligand and SBH (200 μM) and (3) LTα (0.1 μg/ml) and DMSO. Beta-actin (β-actin) was used as loading controls. Western blots are representative of three independent experiments. (b) Quantification of the western blots in (a) by densitometry. Quantified band intensity values are means ± *SD* from three independent experiments. Data are normalized to cells treated with DMSO in the absence of ligand. ***$p < .001$ and ****$p < .0001$ versus control by two-tailed unpaired *t* test. (c) NF-κB activation luciferase activity in HEK293 cells transfected with luciferase reporter plasmids and treated with DMSO in the absence and presence of LTα (0.1 μg/ml). ****$p < .0001$ versus no ligand control by two-tailed unpaired t test. (d) Treatment of increasing doses of SBH (0.1–200 μM) to the NF-κB activation luciferase assay in the absence of LTα. Data are means ± *SD* of three independent experiments

is very similar and the effective concentrations of SBH in the functional assays are consistent with the FRET results.

2.3 | SBH binds TNFR1 and requires the receptor for activation

To determine if SBH directly binds and acts on TNFR1, we first performed affinity measurements using surface plasmon resonance (SPR). Purified TNFR1 ECD was immobilized onto the SPR chip and SBH was flowed through the chip to allow for binding. From the SPR measurements, SBH illustrates dose-dependent binding to the TNFR1 ECD with K_d of 75 μM (Figure 3a, S2), which is lower affinity than the cell-based functional assays. This reduction could be due to: (a) a preference of SBH for the backbone conformation when the receptor is dimerized—the small molecules were selected in the FRET screen based on binding to the dimer; and (b) the likelihood that the SPR experiments have more monomer present than in the plasma membrane of the cells—the immobilized TNFR1 on the SPR chip is most likely a mixture of monomer and dimer equilibrium with a majority of the population being monomer. While we have not quantified the monomer:dimer ratio on the SPR chip, the concentration we used in the immobilization of the TNFR1 ECD was 800 nM (following the company protocol) and we note that the binding affinities of the TNF receptor dimeric interactions were estimated to be in the single-digit micromolar range (~1–9 μM).[30] The concentration of TNFR1 in the plasma membrane is unknown. Beyond this, the difference in affinity and EC_{50} may also be due to the removal of the TNFR1 ECD from its native environment and the likely roles played by the transmembrane domain, cytosolic domains and membrane lipids in increasing the affinity of the dimer,[37,39] all absent in the SPR experiment.

To make sure that the functional effect observed was not due to any nonspecific interactions between SBH and downstream signaling molecules in the NF-κB pathway, we used both parental wild-type (WT) and TNFR1 knockout (KO) HAP1 cell lines (established by CRISPR) to

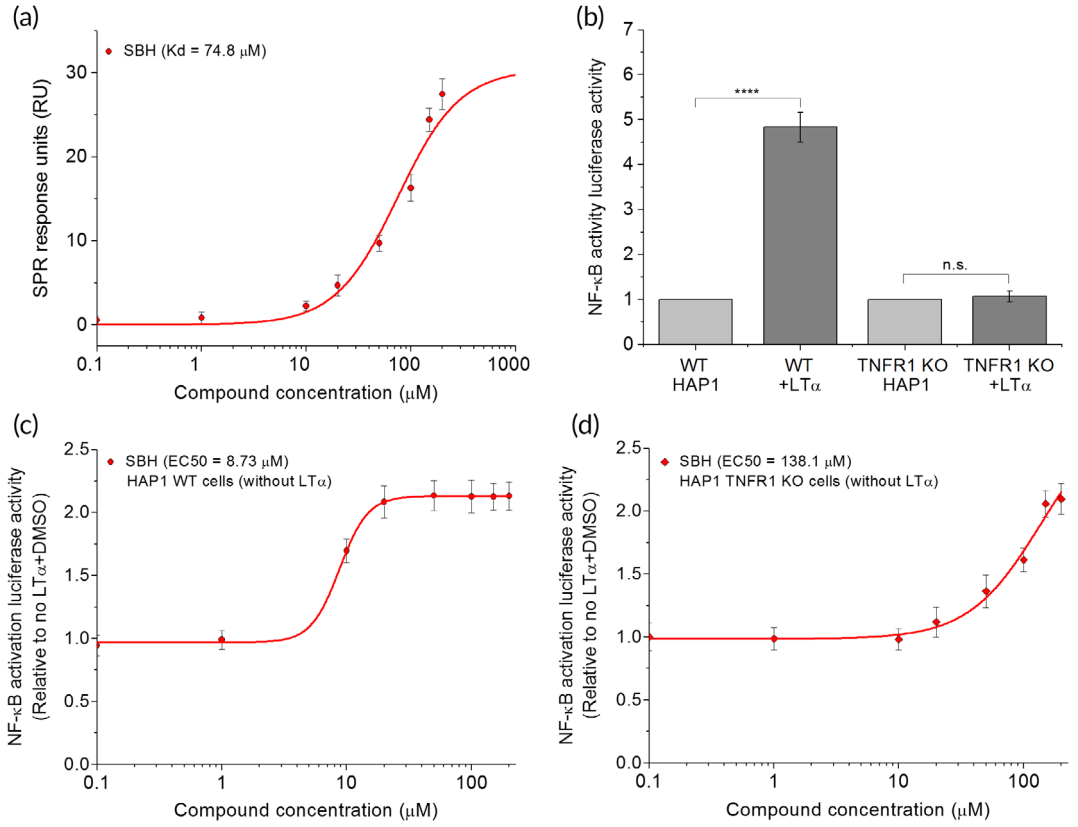

FIGURE 3 SBH binds TNFR1 and requires the receptor for its functional effect. (a) Direct binding of SBH to the TNFR1 extracellular domain (ECD) was characterized by surface plasmon resonance (SPR). Data are means ± *SD* from three independent experiments. (b) NF-κB activation luciferase activity in WT and TNFR1 KO HAP1 cells in the absence and presence of LTα treatment (0.1 μg/ml). Data are means ± *SD* of three independent experiments. ****$p < .0001$ versus control by two-tailed unpaired *t* test and n.s. indicates not significant. (c,d) NF-κB activation luciferase activity in (c) HAP1 WT cells and (d) HAP1 TNFR1 knockout (KO) cells treated with increasing concentration of SBH in the absence of LTα. Data are means ± *SD* of three independent experiments

determine whether the receptor is required for the functional effects of SBH and confirm the compound specificity. In our previous work, we have established that the basal activation of the NF-κB pathway (approximately 20% relative luciferase activity) in the TNFR1 KO HAP1 cells allows them to be used as a first control to ensure that the functional effects we observe in the HEK293 cells are due to direct interactions with TNFR1.[32] Here, we recapitulate that the TNFR1 KO HAP1 cells have basal activation of the NF-κB pathway and are not functionally sensitive to ligand stimulation of TNFR1 (Figure 3b). Again, SBH stimulated NF-κB activation in the absence of the ligand in the WT HAP1 cells to very similar extent as was observed in the HEK293 cells (EC_{50} value = 8.7 μM) (Figure 3c). On the other hand, SBH increased the basal level of NF-κB activation in the TNFR1 KO cells in the absence of ligand at a high EC_{50} value (138 μM), which is more than 10-fold higher than its EC_{50} value in the WT cells (Figure 3d), suggesting that SBH is a specific activator of TNFR1 at its effective concentration.

One additional caveat to this result in the HAP1 cells is that SBH is a known selective inhibitor of 5-HT2C/2B serotonin receptor, though it also inhibits 5-HT2A to some extent.[50] 5-HT2A serotonin receptor activation has been shown to potently suppress TNFα-induced inflammation in cells and animal models.[51,52] This raises the possibility that SBH may be inhibiting the 5-HT2A receptor, lifting its suppression of TNFα activity and thereby increasing NF-κB activation. These effects were restricted to 5-HT2A receptors, as 5-HT2B and 5-HT2C receptor-selective agonists were ineffective in suppressing TNFα-induced inflammation.[53] However, it has been shown that HEK293 cells contain little or no 5-HT2A/2B/2C receptors.[54–57] HAP1 cells, which are near-haploid and have one copy of almost every chromosome, do contain these receptors.[58] Therefore, the effect shown in Figure 3d at high concentrations of SBH in HAP1 TNFR1 KO cells could be due to the inhibition of 5-HT2A receptors.

2.4 | SBH does not alter the binding affinity of the ligand for TNFR1

Since SBH directly binds TNFR1 to activate the receptor in the absence of ligand, we wanted to test if SBH acts as a ligand mimic and disrupts ligand–receptor interaction. We first determined if SBH blocks ligand binding by using co-immunoprecipitation (co-IP) and SPR techniques to monitor ligand–receptor binding in the absence and presence of SBH. Western blot analysis of co-IP experiments showed that SBH did not abolish ligand-receptor interactions (Figure 4a,b). To quantitatively elucidate the noncompetitive nature of the compounds, SPR measurements were conducted by flowing both LTα (50 nM) and SBH (200 μM) through the TNFR1 ECD immobilized surface, and individual treatment of ligand-only or SBH-only served as controls. The response from LTα and SBH co-treatment was equal to the summation of individual contributions by ligand-only and SBH-only binding, indicative of the simultaneous binding of both LTα and SBH to the receptor (Figure 4c). Next, we sought to determine if SBH affected ligand binding affinity through investigating the dose-dependence of ligand binding to TNFR1 in the presence of SBH. Consistent with previously reported results, the binding affinity of LTα was 41 nM (Figure 4d) in dimethyl sulfoxide (DMSO) control.[32,59] In addition, the LTα binding affinity was 39 nM under saturating SBH concentration (200 μM) (Figure 4e), which did not differ significantly from the DMSO control (Figure 4f). We also showed that SBH did not alter soluble TNFR1 PLAD-PLAD interaction while a known competitive inhibitor (zafirlukast) did, confirming that it does not affect receptor dimerization (Figure S3). Although SBH did not directly block ligand binding to the receptor, it remains possible that it is binding elsewhere on TNFR1 to induce its activation. However, our results suggest that SBH may not be behaving like a ligand mimic and not acting through similar mechanisms or binding sites as the native ligand. Hence, it may be stimulating TNFR1 through a noncompetitive mechanism such as altering the receptor conformational activation states. Since purified protein and HEK293 cells, which do not contain serotonin receptors, were used in these mechanistic assays, a saturation dose of SBH (200 μM) was used to ensure we were maximizing the possible effect of the compound.

2.5 | SBH perturbs TNFR1 conformational dynamics

To investigate whether SBH perturbs TNFR1 receptor conformational dynamics, we used previously engineered TNFR1 FRET biosensors with mutations (Q107A, S108A, QS107/108AA, M80A, and V90A [control]) in regions of the ECD that we have predicted with computational models to be the conformationally active region of the receptor.[35] We have recently established experimentally that these residues form a critical region in the conformational network within the ECD that mediates signal propagation from the membrane-distal domain to the membrane-proximal domain of the receptor.[32] In particular, by breaking hydrogen bonds via mutation, we can decouple conformationally linked domains in the ECD, thereby reducing the ability of small molecules to induce

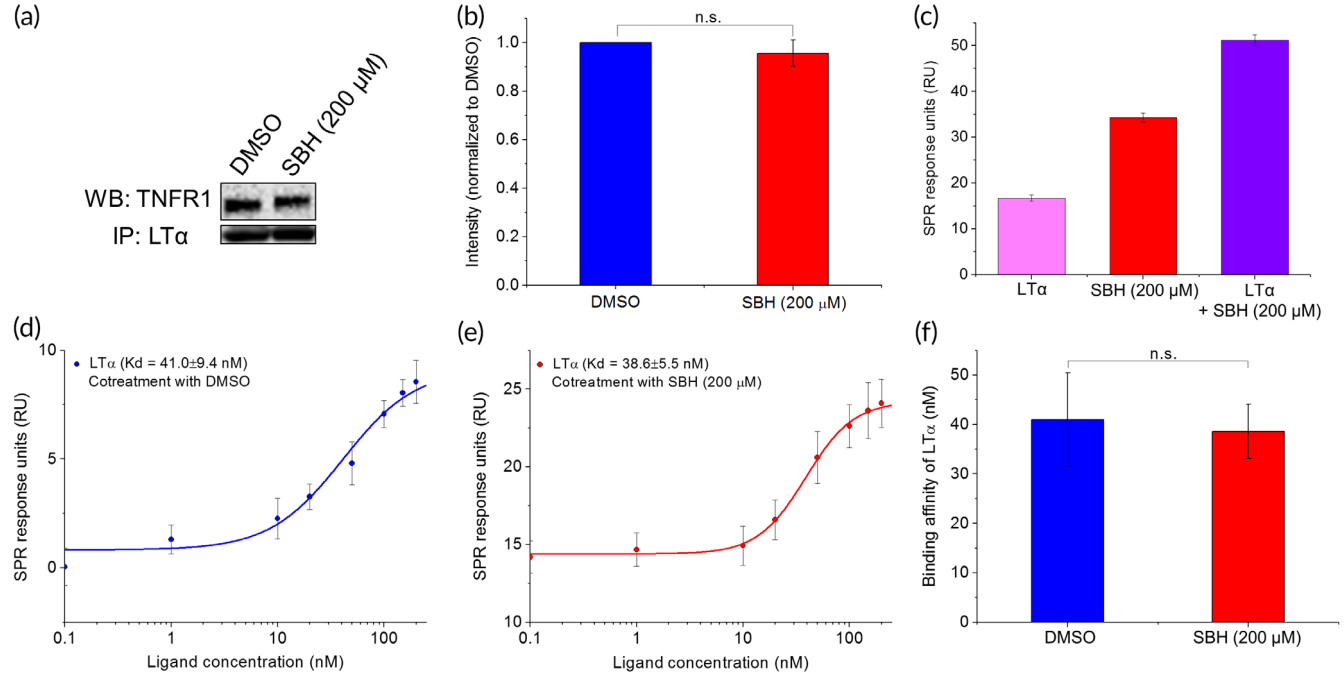

FIGURE 4 SBH does not affect ligand binding affinity to TNFR1. (a) Co-immunoprecipitation between TNFR1 and LTα with treatment of SBH at a saturation dose of 200 μM. The equal amount of LTα is shown as pull-down controls. Western blots are representative of three independent experiments. (b) Quantification of western blots of co-immunoprecipitation results in (a). (c) Noncompetitive binding assay of LTα (50 nM) and SBH (200 μM) to TNFR1 ECD was performed by SPR. Data are means ± *SD* of three independent experiments. (d) Dose-dependent binding of LTα to TNFR1 ECD with an increasing concentration of ligand (0.1–200 nM) in the presence of DMSO. Data are means ± *SD* of three independent experiments. (e) Dose-dependent binding of LTα in the presence of SBH at a saturated compound concentration of 200 μM. Data are means ± *SD* of three independent experiments. (f) Comparison of the binding affinity of LTα to TNFR1 in the absence and presence of SBH. Data are means ± *SD* of three independent experiments and n.s. indicates not significant by two-tailed unpaired *t* test

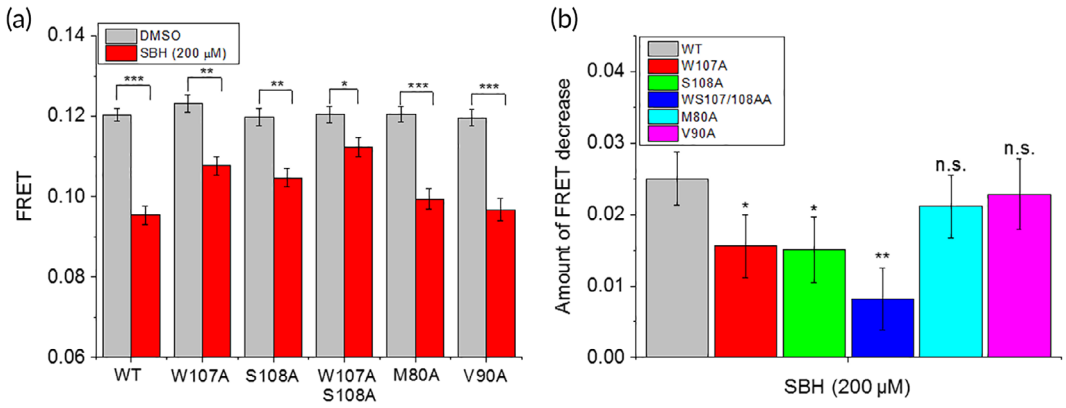

FIGURE 5 SBH perturbs TNFR1 conformational dynamics. (a) SBH (200 μM) reduced FRET significantly in the TNFR1 mutant biosensors (W107A, S108A, WS107/108AA, M80A, and V90A (control)). (b) Comparison of the amount of FRET decreased between HEK293 cells expressing WT and mutant TNFR1 FRET biosensors (W107A, S108A, WS107/108AA, M80A, and V90A) treated with SBH (200 μM) in the absence of ligand. Data are means ± *SD* of three independent experiments. *$p < .05$, **$p < .01$, ***$p < .001$ and n.s. indicates not significant by two-tailed unpaired *t* test

functionally requisite, long-range conformational changes in the full receptor.[32] In studying the conformational effects of SBH binding to the ECD using FRET we are looking directly at the effect of the small molecule on the structure of the receptor. Thus, we do not believe that downstream or alternate signaling machinery is likely to influence our observed FRET changes, even at high concentrations of SBH. First, we still observed significant

FRET reduction in the mutant FRET biosensors upon SBH (200 μM) treatment (Figure 5a), indicating that SBH still binds and perturbs the mutant TNFR1. Interestingly, however, there was a significant decrease in the magnitude of the FRET change with treatment of SBH, especially in the W107A, S108A, and W107A/S108A mutant biosensors (Figure 5b). This likely reflects a loss in conformational coupling across the ECD needed to open the receptor. As a negative control, we found that the change in FRET relative to wild type was negligible in a V90A mutant, a site that is far from the dynamic centers in the ECD (Figure 5a,b). Our results showed that the propensity of decoupling the conformationally active domains is significant in W107A and S108A mutations with the W107A/S108A double mutant having the strongest (likely additive) effect, but no effect in the M80A mutant. The lack of an effect in M80A is consistent with our previous computational study which predicted that the major effect of ligand binding on receptor dynamics is in the 107–113 region of the ligand-binding loop (with stronger coupling due to hydrogen bond connectivity), with a much smaller effect in the 77–81 region.[35] However, we do note that in our previous study of TNFR1 inhibitors we did see an effect of the M80A mutant,[32] perhaps suggesting different structural coupling for the two distinct conformational changes associated with activation and inhibition.

One caveat to mention here is the possibility that the reduced FRET in Figure 5a,b could be an artifact of reduced SBH binding (if e.g., the SBH binding site involves the mutated residues), though we do not believe this to be the case. First, the mutations used in this study are all key native ligand-binding residues. We have shown that SBH does not affect ligand binding to the receptor (Figure 4), suggesting that SBH does not bind to these residues (as it would cause steric hindrance to ligand binding). Furthermore, we would expect that the FRET change would be totally abolished if these residues are part of the binding site of SBH, though it is, of course, possible that the mutations reduce SBH affinity without totally eliminating binding. Absolute clarity on these points will require higher-resolution structural and dynamic characterization (e.g., using NMR) to be pursued in future studies.

2.6 | Synergistic effect of SBH and ligand on stimulating TNFR1 signaling

Since SBH alters the conformational states of TNFR1 and does not block LTα binding to TNFR1, we investigated the functional effect of SBH in the presence of ligand in HEK293 cells. We hypothesize that if both SBH and LTα are binding TNFR1 and simultaneously activating the receptor through separate mechanisms, the functional effect with co-treatment of SBH and LTα will be additive. In contrast, if we could show that the functional effect from the co-treatment of SBH and LTα is greater than the sum of their individual effect, then this would highlight the possibility that subtle changes in conformation of the preassembled dimer may be sufficient to switch the activating potential of the receptor from a basal activation state (triggered by LTα only without SBH) to an activation state with higher signaling efficiency (triggered by both LTα and SBH) in the ligand-bound, fully assembled state.

Strikingly, co-treatment of LTα and increasing doses of SBH in HEK293 cells illustrated a twofold increase in the NF-κB activation luciferase activity (from an intensity of 6 with LTα-only treatment to 12 with LTα and SBH co-treatment) with a similar EC_{50} of 5.3 μM (Figure 6a), instead of having an additive effect (a total intensity of 8 that is a sum of 6 [LTα-only] and 2 [SBH-only]). A similar activation profile was also observed with co-treatment of LTα and SBH in HAP1 WT cells with an EC_{50} of 9.0 μM (Figure 6b). On the other hand, SBH increased the basal level of NF-κB activation in the TNFR1 KO cells in the presence of ligand at a high EC_{50} value (124 μM), which was more than 10-fold higher than its EC_{50} value in the WT cells (Figure 6c). We tested the synergistic effect between SBH and LTα at 20 μM of SBH and illustrated that the effect was only observed in the WT cells but not in the TNFR1 KO cells, thus confirming the compound specificity to TNFR1 (Figure 6d). We also observed consistent synergistic effect of LTα and SBH in IκBα degradation assay where the cells treated with both LTα and SBH showed a further twofold degradation of IκBα as compared to the cells with LTα-only treatment (Figure S4A,B) and in a dose-dependent manner with an EC_{50} of 38 μM (Figure S4C,D). We also investigated if SBH alters the functional EC_{50} of the ligand by treating the cells with increasing doses of LTα (0.001–5 μg/ml) in the absence and presence of SBH (200 μM). Treatment with LTα only in the presence of DMSO showed a functional EC_{50} of 14 ng/ml (Figure 6e) while co-treatment of LTα and SBH showed an EC_{50} of 17 ng/ml (Figure 6f). A comparison between the functional EC_{50} values illustrated that they are not significantly different (within error of measurements) (Figure 6g), indicating that treatment of SBH did not enhance the functional effect of LTα which is consistent with the SPR data showing that the ligand binding affinity to receptor was not changed (Figure 4f). These results suggest a synergistic

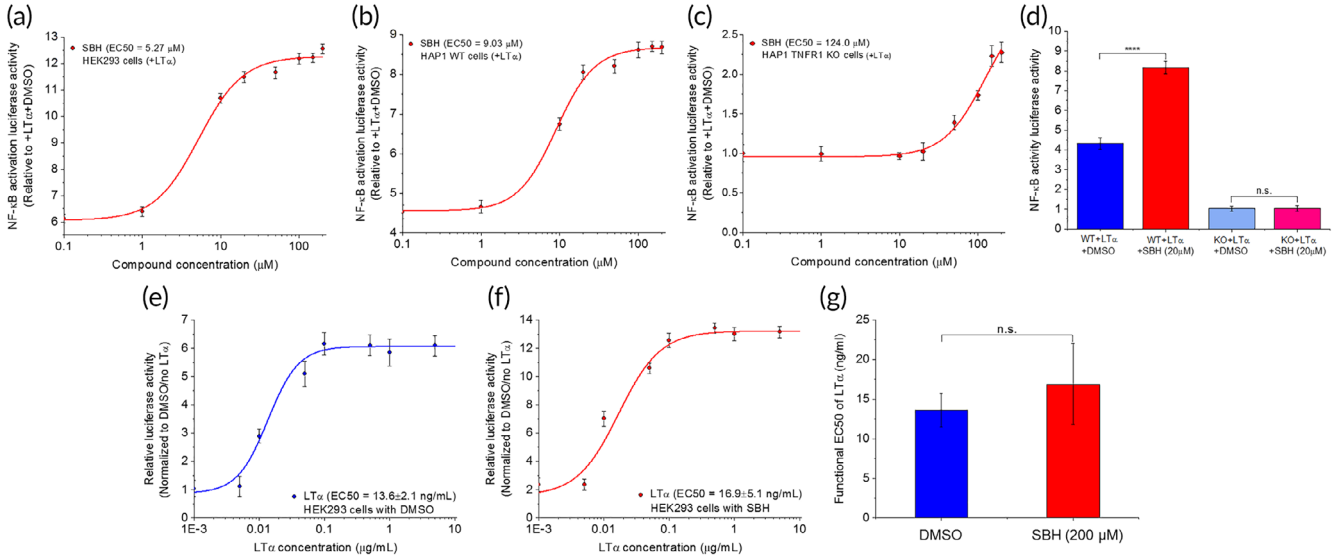

FIGURE 6 Synergistic effect of SBH and LTα on TNFR1-stimulated NF-κB activation. (a–c) NF-κB activation luciferase activity in (a) HEK293 cells, (b) HAP1 WT cells, and (c) HAP1 TNFR1 knockout (KO) cells treated with LTα (0.1 μg/ml) and increasing concentrations of SBH (0.1–200 μM). Data are means ± *SD* of three independent experiments. (d) Synergistic effect of SBH and LTα tested at 20 μM, a TNFR1-specific compound concentration. (e) Dose-dependent functional effect of LTα in stimulating TNFR1-induced NF-κB activation in HEK293 cells with increasing concentration of ligand (0.001–5 μg/ml) in the presence of DMSO. Data are means ± *SD* of three independent experiments. (f) Dose-dependent functional effect of LTα in the presence of SBH at a saturated compound concentration of 200 μM. Data are means ± *SD* of three independent experiments. (g) Comparison of the functional effect of LTα in the absence and presence of SBH (200 μM). Data are means ± *SD* of three independent experiments and n.s. indicates not significant by two-tailed unpaired *t* test

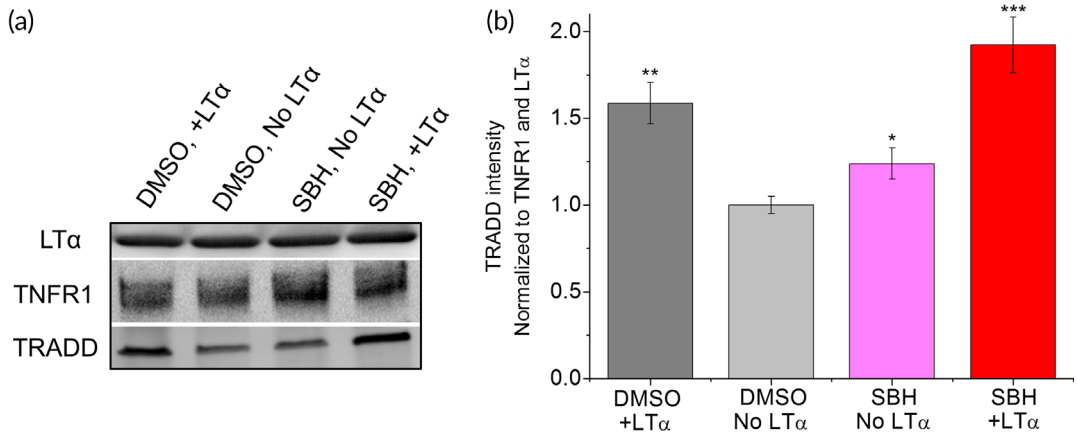

FIGURE 7 Conformational states of TNFR1 as a molecular switch for receptor function. (a) Co-immunoprecipitation (co-IP) between LTα, TNFR1, and TRADD with and without treatment of SBH (200 μM) and in the absence and presence of the ligand (0.1 μg/ml). The equal amount of FLAG-tagged LTα coated on the magnetic beads with the FLAG antibody is shown as pull-down controls. Western blots are representative of three independent experiments. (b) Quantification of the western blot for co-IP in (a). Data are means ± *SD* from three independent experiments. *$p < .05$, **$p < .01$ and ***$p < .001$ versus control by two-tailed unpaired *t* test

effect of SBH and LTα in stimulating TNFR1 signaling by forcing the receptor into an open conformation that sensitizes the receptor for more efficient (twofold) signal transduction in both the absence and presence of ligand stimulation.

2.7 | Conformational states of TNFR1 as a molecular switch for receptor function

As we have shown, SBH reduces FRET in the TNFR1 biosensor—corresponding to the receptor adopting an

open conformation—and subsequently stimulates receptor signaling. To explain how conformational states of TNFR1 could dictate receptor function, we hypothesize that receptor conformational states may determine its accessibility to the signaling machinery, that is, the recruitment of the downstream signaling molecules. To test this, we performed another co-IP experiment to determine the interactions between TNFR1 and TRADD (TNFR1 associated death domain) in the absence and presence of SBH (200 μM) in HEK293 cells. The co-IP results show that significantly more TRADD is pulled down with the treatment of SBH either in the absence or presence of the ligand (Figure 7a,b). Thus, SBH operates by facilitating a conformational opening of TNFR1 that enhances the recruitment of TRADD.

3 | DISCUSSION

Being a major contributor to the NF-κB activation pathway, TNFR1 activation can lead to increased NF-κB activation as a treatment of immune deficiency and neurodegenerative diseases.[60,61] To the best of our knowledge, SBH is both the first-known small molecule activator of TNFR1 and the first activator that acts through perturbing receptor conformational states. This conformational selection activates TNFR1 in the absence of ligand and increases the magnitude of ligand-induced stimulation without competing with the ligand-binding site. This receptor-specific mechanism is different from the existing activators for other TNF receptors that either sensitize receptors to ligand activation or mimic ligand, as in each of those cases the activation efficiency is limited by the competition with ligand binding. In addition, in the case of TNFR1, blocking of ligand binding would increase the free concentration of ligand, which may then over-stimulate TNFR2 that implicates cell death.[62–64] Current TNF receptor-specific small molecule activators include compounds that sensitize FAS receptor to its agonist antibody for killing of cancer cells,[16] small molecule mimic of Smac that potentiates TRAIL and TNFα-mediated deaths in cancer cells,[17] another small molecule (bioymifi) that can act as a single agent to induce DR5 clustering and aggregation, leading to apoptosis, similar to TRAIL mimics targeting DR5 for cancer therapy[18] and compounds that block OX40–OX40L interactions by acting as OX40 agonist/ligand.[19]

Here, we would like to clarify that SBH works differently from these small molecules in that even though it activates TNFR1 in the absence of ligand, it does not behave as ligand mimic to compete with cognate ligand binding. In addition, the effect of co-treatment of LTα and SBH is more than the sum of the individual effect from LTα-only or SBH-only treatment. For example, regardless of receptor constitutive signaling in the absence of ligand or ligand stimulation, the receptor activation is estimated to be increased by twofold such as the relative luciferase activity changed from 1 to 2 (in the absence of ligand) or 6 to 12 (in the presence of ligand) rather than being additive. This indicates that the receptor is adopting an active conformation that sensitizes the receptor to amplify twice the activation signals, thus behaving differently as the currently known TNF receptor activators.

SBH exerts its activation effect by altering the conformational state of the preassembled dimer to adopt an open and active conformation. This is consistent with our previous computational study showing that ligand activation of TNFR1 adopts an opening conformation.[35] This is further supported by other studies on TNF receptors have also shown that opening conformations were adopted and preferred for receptor activation.[37,38] From the perspective of understanding the mechanism of TNFR1 activation, this demonstrates that TNFR1 can be increasingly active when both the ligand is bound and the receptor dimer is intact. In addition, our TNFR1-TRADD co-IP results showed that receptor open conformation allows increasing accessibility of TRADD in binding to the TNFR1 death domain. This suggests the need to take into account the three-dimensional spatial orientation of the receptor to further understand its activation mechanism. This new hypothesis would also require higher resolution microscopic or biophysical techniques in studying receptor orientations beyond the two-dimensional axis. Putting these together, we suggest that the ensemble of TNFR1 conformational activation states can be stabilized by small molecules for differential receptor function, acting like a molecular switch.

4 | MATERIALS AND METHODS

4.1 | Molecular biology

In our previous work, we generated the DNAs (TNFR1ΔCD-GFP and TNFR1ΔCD-RFP) used in the engineering of the TNFR1 FRET biosensor.[31] Briefly, standard cloning techniques were used to fuse cDNAs encoding truncated TNFR1ΔCD (amino acids 1–242) with the N-terminus of the EGFP and TagRFP vectors. Quikchange mutagenesis (Agilent Technologies, Santa Clara, CA, USA) was used to introduce the mutations of the key ligand-binding residues (Q107A, S108A, QS107/108AA, and M80A) and the control mutant (V90A) in the TNFR1ΔCD-GFP and TNFR1ΔCD-RFP plasmids. All vectors contain the monomeric mutation A206K to the fluorescent proteins in order to prevent constitutive fluorophore clustering.[65] All plasmid sequences were confirmed by Sanger sequencing.

4.2 | Cell culture and generation of stable cell lines

Human embryonic kidney cells 293 (HEK293, ATCC, Manassas, VA, USA) were cultured in phenol red-free Dulbecco's Modified Eagle Medium (Gibco, Billings, MT, USA), supplemented with 100 μg/ml streptomycin (Gibco), 100 U/ml penicillin, 2 mM L-Glutamine (Invitrogen, Carlsbad, CA, USA), and 10% heat-inactivated fetal bovine serum (FBS HI, Gibco). HAP1 wild-type and TNFR1 knockout cells (Horizon Discovery, Lafayette, CO, USA) were cultured in Iscove's Modified Dulbecco's Medium (Gibco), supplemented with 100 μg/ml streptomycin (Gibco), 100 U/ml penicillin and 10% heat-inactivated FBS (FBS HI, Gibco). An incubator with 5% CO_2 (Forma Series II Water Jacket CO_2 Incubator, Thermo Scientific, Coon Rapids, MN, USA) at 37°C was used to maintain the cell cultures. CRISPR/Cas technology was used to generate the HAP1 TNFR1 knockout cell line containing a 70 base pair insertion in a coding exon of TNFRSF1A. To confirm the knockout in the cells, Sanger sequencing was performed as a quality control. Our previous work describes how the TNFR1ΔCD-FRET pair and TNFR1ΔCD-GFP stable cell lines were generated.[31] These stable cell lines have been monitored continuously for over 4 years while maintaining expression above 95% characterized by flow cytometry.[31] The TNFR1ΔCD-FRET pair in the stable cell line shows high expression, which indicates that they are functional and applicable in HTS. HEK293 cells were transiently transfected using Lipofectamine 3000 (Invitrogen) with TNFR1ΔCD-GFP and TNFR1ΔCD-RFP DNAs containing the respective mutations (Q107A, S108A, QS107/108AA, M80A, and V90A) in order to generate the mutant forms of the TNFR1 FRET biosensor.

4.3 | HTS with LOPAC library

The LOPAC library containing 1,280 compounds was purchased from Millipore Sigma (Madison, WI, USA) and an FX liquid dispenser was used to format the compounds into 96-well mother plates. An Echo liquid dispenser was used to subsequently format across four plates of the 384-well plate at 50 nl (10 μM final concentration per well). DMSO was loaded in columns 1, 2, 23, and 24 (negative controls) as well as matching %v/v as in-plate no-compound controls. The assay plates chosen were the 384-well flat, black-bottom polypropylene plates (PN 781209, Greiner Bio-One, Monroe, NC, USA) because of their low inter-well cross-talk and low autofluorescence. The plates were then sealed and stored at −20°C. The triplicate screens were performed with a library screened a day over three different days. Fresh vial of TNFR1ΔCD-GFP/RFP (TNFR1ΔCD-FRET pair) and TNFR1ΔCD-GFP (donor-only control) cells were thawed, plated in 225 cm^2 flasks (Corning, Corning, NY, USA) and checked for expression 3 days prior to screening. The cells were then expanded into six 225 cm^2 flasks for 3 days. The stable cells were harvested to check for expression and response variation in fluorescent intensity prior to each day of screening. The stable cells were then dispensed into the drug plates (50,000 cells/well) and incubated with the compounds or DMSO as a negative control. The fluorescence waveforms of the plates and the lifetime of the samples were then acquired using a prototype fluorescence lifetime plate-reader (Fluorescence Innovations, Inc., Minneapolis, MN, USA) as described.[31]

4.4 | Data analysis for HTS

Using least-squares minimization global analysis software (Fluorescence Innovations, Inc.), time-resolved fluorescence waveforms obtained from each well were fitted to single-exponential decays. This was done to obtain a donor–acceptor lifetime (τ_{DA}) from the TNFR1ΔCD-GFP/RFP (FRET pair) cell line and donor lifetime (τ_D) from a TNFR1ΔCD-GFP donor-only control cell line. Equation (1) was used to calculate FRET efficiency (E).

$$E = 1 - \left(\frac{\tau_{DA}}{\tau_D}\right) \quad (1)$$

Using SBH as a positive control and DMSO as a negative control, an HTS assay quality indicator (the Z-factor) was calculated based on Equation (2) 66.

$$Z' = 1 - \frac{3(\sigma_p + \sigma_n)}{|\mu_p - \mu_n|} \quad (2)$$

where σ_p and σ_n are the SDs of the observed τ_{DA} values, and μ_p and μ_n are the mean τ_{DA} values of the positive and negative controls, respectively. We utilized the median and normalized median absolute deviation (1.4826 × MAD) in place of the mean and SD, respectively, to make this metric less sensitive to strong outliers.[67] The Z-factor obtained using SBH as a positive control was 0.55 ± 0.02, which indicates excellent assay quality.

Based on the analysis of the spectral waveforms of each well from the LOPAC screen, fluorescent compounds were determined to be potential false positives

due to interference from compound fluorescence by a set of stringent fluorescent compound filters.[68] After the fluorescent compounds and potential false positives were removed, a histogram of the FRET distribution from all compounds in the screen was plotted. This histogram was fitted to a Gaussian curve to obtain a mean and *SD*. A compound that changed the FRET efficiency by more than four times the standard deviation (4*SD*) relative to the mean was defined as a hit.

4.5 | FRET dose–response assay

The three hit compounds, SB 200646 hydrochloride (SBH) (S0568), candesartan cilexetil (CC) (SML0245), and palmitoyl-DL-carnitine chloride (PDLCC) (P4509) were purchased from Millipore Sigma. Each drug compound was dissolved in DMSO to make a 10 mM stock solution. Each solution was then serially diluted in 96-well mother plates to obtain eight doses at 50× concentrations. Hits were screened at eight different concentrations (0.1–200 μM). Using a Mosquito HV liquid handler (TTP Labtech Ltd.), 1 μl of compounds were transferred from the mother plates into assay plates. The same HTS methods were used on the cell preparation of the wild-type TNFR1 FRET biosensor in the FRET dose-response assays.

4.6 | Functional assays (IκBα degradation assay and NF-κB activation assay)

IκBα degradation assays with HEK293 cells were performed with Western blots as described[31] and the blots were quantified by densitometry using ImageJ. β-actin was used as a loading control and the data were normalized to the amount of IκBα and the respective controls. The NF-κB activation luciferase assays were conducted by transfecting NF-κB-luciferase reporter genes (10 μg of firefly luciferase genes and 1 μg of *Renilla* luciferase genes) in a 100 mm plate containing HEK293, HAP1 wild-type or TNFR1 knockout cells using Lipofectamine 3000 (Invitrogen). After 48 hr, the transfected cells were harvested and dispensed into 96-well assay plates (30,000 cells/well, total volume 50 μl) and incubated with SBH (0.1–200 μM) or DMSO (negative control) in both the presence (0.1 μg/ml) and absence of LTα for 18 hr at 37°C. To test the functional EC_{50} of the ligand, HEK293 cells were treated with increasing doses of LTα (0.001–5 μg/ml) in the absence and presence of SBH (200 μM). Readings for luciferase activities were recorded after 24 hr. To take the luciferase measurements, Dual-Glo Luciferase Reagent (Promega, Fitchburg, WI, USA) (50 μl) was added and incubated at room temperature for 15 min. The firefly luminescence was first measured using a Cytation 3 Cell Imaging Multi-Mode Reader luminometer (BioTek, Winooski, VT, USA). This was followed by the addition of Dual-Glo Stop & Glo Reagent (Promega) (50 μl) and incubated at room temperature for another 15 min. The *Renilla* luminescence was then measured using a luminometer. The luciferase activity was normalized to the *Renilla* activity, which serves as a control and further normalized to the respective controls.

4.7 | Mechanistic assays

Co-immunoprecipitation between endogenous TNFR1 and ligand LTα in the presence and absence of SBH was carried out as described.[31] Briefly, lysates of HEK293 cells containing endogenous TNFR1 and anti-FLAG magnetic beads coated with FLAG-tagged LTα were prepared. The cell lysates containing TNFR1 and magnetic beads coated with LTα were then incubated in the presence of DMSO (control) or SBH (activator, 200 μM). After 24 hr, the proteins were eluted from the magnetic beads using glycine pH 2.5 and Western blots were performed using FLAG (2368S, Cell Signaling Technology, Danvers, MA, USA) and TNFR1 (sc-8436, Santa Cruz Biotechnology, Santa Cruz, CA, USA) antibodies. Images were quantified by ImageJ for densitometry analysis. The purification of the FLAG-tagged LTα and the FLAG-tagged TNFR1 PLAD (residues 30–82) were performed as described previously.[31] Under native conditions, the soluble PLAD protein was shown to exist as dimers.[31] The recombinant human TNFR1 ECD was purchased (Abcam, Cambridge, MA, USA). SDS-PAGE 4–15% gels (Bio-Rad, Hercules, CA, USA) were used to assess the purity of proteins under reducing conditions followed by Coomassie staining. The BCA assay (Thermo Fisher Scientific, Waltham, MA, USA) was used to measure protein concentrations. To test the disruption of receptor-receptor, purified soluble TNFR1 PLAD (5 μg) were assessed by Native-PAGE gels (Bio-Rad) in the presence of DMSO, SBH (200 μM) or zafirlukast (200 μM) under nonreducing conditions followed by Coomassie staining.

4.8 | SPR binding assay

A BIAcore S200 was used to perform SPR analysis to determine the binding affinity between TNFR1 ECD and compounds or ligand. Using amine coupling, the recombinant human TNFR1 ECD (Abcam) was immobilized on the CM5 sensor chip (GE Healthcare, Waukesha, WI, USA). Briefly, the dextran surface was activated with 0.4 M

1-ethyl-3-(3-dimethylaminopropyl)carbodiimide hydrochloride and 0.1 M *N*-hydroxysuccinimide in a 1:1 mixture. TNFR1 ECD (20 μg/ml) in 10 mM sodium acetate at pH 5 was then flowed past a working surface for immobilization. The remaining activated carboxymethyl groups were then blocked with 1 M ethanolamine at pH 8.5. The immobilization was set to reach a level of 2500 RU suitable for binding analysis. The reference surface was activated and reacted with only ethanolamine as a control.

Compound SBH at eight different concentrations (0.1–200 μM) as well as DMSO-only controls were prepared in HEPES-EP containing a total of 2% DMSO for the direct binding assays between the receptor and the small molecules. To test the competition between LTα and SBH, ligand at 50 nM was prepared in HEPES-EP in the presence of a saturated dose of SBH (200 μM) or DMSO containing a total of 2% DMSO. To investigate the effect of SBH on ligand binding affinity, increasing doses of LTα (0.1–200 nM) were prepared in HEPES-EP in the presence of a saturated dose of SBH (200 μM). The samples were injected over both the reference and ECD immobilized surfaces at 10 μl/min for 90 s and dissociated in glycine-HCl with a pH of 2.5. Along with blanks from buffer and DMSO-only controls, all the samples were measured on a 96-well microplate (GE Healthcare) at 25°C. To determine the steady-state binding, reflectivity response units were extracted from response curves 5 s prior to the end of the injection. Acquired data were double referenced with blanks and DMSO using standard procedures using Biacore S200 Evaluation Software v1.0.

4.9 | TRADD recruitment assay

HEK293 cells were cultured in 100 mm plates at 5 million cells per plate. Respective SBH (200 μM) and ligand treatments (0.1 μg/ml) were then performed and incubated for 24 hr. The cells were then harvested and lysed. Anti-FLAG magnetic beads were pre-coated with FLAG-tagged LTα for 24 hr. After 24 hr, the LTα bound beads were washed with PBS for three times and further incubated with the supernatant of the cell lysates for another 24 hr for the pulled down of TNFR1 and TRADD (which was recruited to the receptor). After incubation, the beads were washed with PBS for three times and the bound proteins were eluted using 30 μl of glycine pH 2.5. The protein samples were then mixed with the 4× loading dye with β-mercaptoethanol reducing agent and Western blots were performed using FLAG (2368S, Cell Signaling Technology), TNFR1 (sc-8436, Santa Cruz Biotechnology), and TRADD (3684S, Cell Signaling Technology) antibodies. The Western blots were then stained with respective secondary antibodies and images were acquired using the ChemiDoc™ MP Imaging System (Bio-Rad). Images were quantified by ImageJ for densitometry analysis.

4.10 | Statistical analysis

Data are shown as mean ± *SD* unless stated otherwise. A two-tailed unpaired *t* test (Student's *t* test) was used in data analysis to determine the statistical significance for all experiments. The *p* values were determined using GraphPad Software with values of $p < .05$ designated as statistically significant. *p* values were denoted using asterisks in figures following the GraphPad style (*$p < .05$, **$p < .01$, ***$p < .001$, and ****$p < .0001$).

ACKNOWLEDGMENTS

We thank Colin Lim and Zhipeng Ding from the Sachs group, and Samantha Yuen from the Thomas group for technical support. Flow cytometry was performed at the UMN Lillehei Heart Institute, spectroscopy at the UMN Biophysical Technology Center and compound dispensing and surface plasmon resonance (S10 Shared Instrument Grant 1S10OD021539-01 funded by the Office of Research Infrastructure Programs (ORIP)/National Institutes of Health (NIH)) at the UMN Institute of Therapeutic Drug Discovery and Development (ITDD) High-Throughput Screening Laboratory.

CONFLICT OF INTEREST

The authors declare no potential conflict of interest.

AUTHOR CONTRIBUTIONS

C.H.L. and J.N.S. conceived and directed the project. C.H.L. designed and conducted all the experiments. E.C.H. provided technical support for functional and mechanistic assays. C.H.L. and J.N.S. wrote the manuscript.

ORCID

Jonathan N. Sachs https://orcid.org/0000-0003-1403-5960

REFERENCES

1. Locksley RM, Killeen N, Lenardo MJ. The TNF and TNF receptor superfamilies: Integrating mammalian biology. Cell. 2001; 104:487–501.
2. MacEwan DJ. TNF ligands and receptors—A matter of life and death. Br J Pharmacol. 2002;135:855–875.
3. Ashkenazi A, Dixit VM. Death receptors: Signaling and modulation. Science. 1998;281:1305–1308.
4. Wajant H, Scheurich P. TNFR1-induced activation of the classical NF-kappaB pathway. FEBS J. 2011;278:862–876.
5. Brenner D, Blaser H, Mak TW. Regulation of tumour necrosis factor signalling: Live or let die. Nat Rev Immunol. 2015;15:362–374.

6. Chan JK, Greene WC. NF-kappaB/Rel: Agonist and antagonist roles in HIV-1 latency. Curr Opin HIV AIDS. 2011;6:12–18.
7. O'Neill LA, Kaltschmidt C. NF-kappa B: A crucial transcription factor for glial and neuronal cell function. Trends Neurosci. 1997;20:252–258.
8. Cardoso SM, Oliveira CR. Inhibition of NF-kB renders cells more vulnerable to apoptosis induced by amyloid beta peptides. Free Radic Res. 2003;37:967–973.
9. Muriel P. NF-kappaB in liver diseases: A target for drug therapy. J Appl Toxicol. 2009;29:91–100.
10. Manuvakhova MS, Johnson GG, White MC, et al. Identification of novel small molecule activators of nuclear factor-kappaB with neuroprotective action via high-throughput screening. J Neurosci Res. 2011;89:58–72.
11. Kasperczyk H, La Ferla-Bruhl K, Westhoff MA, et al. Betulinic acid as new activator of NF-kappaB: Molecular mechanisms and implications for cancer therapy. Oncogene. 2005;24:6945–6956.
12. Chan JK, Bhattacharyya D, Lassen KG, Ruelas D, Greene WC. Calcium/calcineurin synergizes with prostratin to promote NF-κB dependent activation of latent HIV. PLoS One. 2013;8:e77749.
13. Holden NS, Squires PE, Kaur M, Bland R, Jones CE, Newton R. Phorbol ester-stimulated NF-kappaB-dependent transcription: Roles for isoforms of novel protein kinase C. Cell Signal. 2008;20:1338–1348.
14. Busuttil V, Bottero V, Frelin C, et al. Blocking NF-kappaB activation in Jurkat leukemic T cells converts the survival agent and tumor promoter PMA into an apoptotic effector. Oncogene. 2002;21:3213–3224.
15. Grandison L, Nolan GP, Pfaff DW. Activation of the transcription factor NF-KB in GH3 pituitary cells. Mol Cell Endocrinol. 1994;106:9–15.
16. Schimmer AD, Thomas MP, Hurren R, et al. Identification of small molecules that sensitize resistant tumor cells to tumor necrosis factor-family death receptors. Cancer Res. 2006;66:2367–2375.
17. Li L, Thomas RM, Suzuki H, De Brabander JK, Wang X, Harran PG. A small molecule Smac mimic potentiates TRAIL- and TNFα-mediated cell death. Science. 2004;305:1471–1474.
18. Wang G, Wang X, Yu H, et al. Small-molecule activation of the TRAIL receptor DR5 in human cancer cells. Nat Chem Biol. 2013;9:84–89.
19. Song Y, Margolles-Clark E, Bayer A, Buchwald P. Small-molecule modulators of the OX40-OX40 ligand co-stimulatory protein-protein interaction. Br J Pharmacol. 2014;171:4955–4969.
20. Gómez MI, Seaghdha MO, Prince AS. *Staphylococcus aureus* protein a activates TACE through EGFR-dependent signaling. EMBO J. 2007;26:701–709.
21. Sajjan US, Hershenson MB, Forstner JF, LiPuma JJ. Burkholderia cenocepacia ET12 strain activates TNFR1 signalling in cystic fibrosis airway epithelial cells. Cell Microbiol. 2008;10:188–201.
22. Ma E, Wang X, Li Y, et al. Induction of apoptosis by furanodiene in HL60 leukemia cells through activation of TNFR1 signaling pathway. Cancer Lett. 2008;271:158–166.
23. Valley CC, Lewis AK, Mudaliar DJ, et al. Tumor necrosis factor-related apoptosis-inducing ligand (TRAIL) induces death receptor 5 networks that are highly organized. J Biol Chem. 2012;287:21265–21278.
24. Reis CR, van Assen AHG, Quax WJ, Cool RH. Unraveling the binding mechanism of trivalent tumor necrosis factor ligands and their receptors. Mol Cell Proteomics. 2011;10:M110.002808.
25. Mukai Y, Nakamura T, Yoshikawa M, et al. Solution of the structure of the TNF-TNFR2 complex. Sci Signal. 2010;3:ra83.
26. Vanamee ÉS, Faustman DL. Structural principles of tumor necrosis factor superfamily signaling. Sci Signal. 2018;11:eaao4910.
27. Banner DW, D'Arcy A, Janes W, et al. Crystal structure of the soluble human 55 kd TNF receptor-human TNFβ complex: Implications for TNF receptor activation. Cell. 1993;73:431–445.
28. Chan FK-M, Chun HJ, Zheng L, Siegel RM, Bui KL, Lenardo MJ. A domain in TNF receptors that mediates ligand-independent receptor assembly and signaling. Science. 2000;288:2351–2354.
29. Naismith JH, Devine TQ, Brandhuber BJ, Sprang SR. Crystallographic evidence for dimerization of unliganded tumor necrosis factor receptor. J Biol Chem. 1995;270:13303–13307.
30. Lee H-W, Lee S-H, Lee H-W, Ryu Y-W, Kwon M-H, Kim Y-S. Homomeric and heteromeric interactions of the extracellular domains of death receptors and death decoy receptors. Biochem Biophys Res Commun. 2005;330:1205–1212.
31. Lo CH, Vunnam N, Lewis AK, et al. An innovative high-throughput screening approach for discovery of small molecules that inhibit TNF receptors. SLAS Discov. 2017;22:950–961.
32. Lo CH, Schaaf TM, Grant BD, et al. Noncompetitive inhibitors of TNFR1 probe conformational activation states. Sci Signal. 2019;12:eaav5637.
33. Chan FK-M, Siegel RM, Zacharias D, et al. Fluorescence resonance energy transfer analysis of cell surface receptor interactions and signaling using spectral variants of the green fluorescent protein. Cytometry. 2001;44:361–368.
34. Chan FK-M. Three is better than one: Pre-ligand receptor assembly in the regulation of TNF receptor signaling. Cytokine. 2007;37:101–107.
35. Lewis AK, Valley CC, Sachs JN. TNFR1 signaling is associated with backbone conformational changes of receptor dimers consistent with overactivation in the R92Q TRAPS mutant. Biochemistry. 2012;51:6545–6555.
36. Vunnam N, Lo CH, Grant BD, Thomas DD, Sachs JN. Soluble extracellular domain of death receptor 5 inhibits TRAIL-induced apoptosis by disrupting receptor–receptor interactions. J Mol Biol. 2017;429:2943–2953.
37. Vunnam N, Campbell-Bezat CK, Lewis AK, Sachs JN. Death receptor 5 activation is energetically coupled to opening of the transmembrane domain dimer. Biophys J. 2017;113:381–392.
38. Lewis AK, James ZM, McCaffrey JE, et al. Open and closed conformations of the isolated transmembrane domain of death receptor 5 support a new model of activation. Biophys J. 2014;106:L21–L24.
39. Lewis AK, Valley CC, Peery SL, et al. Death receptor 5 networks require membrane cholesterol for proper structure and function. J Mol Biol. 2016;428:4843–4855.
40. Liu C, Walter TS, Huang P, et al. Structural and functional insights of RANKL-RANK interaction and signaling. J Immunol. 2010;184:6910–6919.
41. Botos I, Segal DM, Davies DR. The structural biology of toll-like receptors. Structure. 2011;19:447–459.

42. Latz E, Verma A, Visintin A, et al. Ligand-induced conformational changes allosterically activate toll-like receptor 9. Nat Immunol. 2007;8:772–779.
43. Vilar M, Charalampopoulos I, Kenchappa RS, et al. Activation of the p75 neurotrophin receptor through conformational rearrangement of disulphide-linked receptor dimers. Neuron. 2009;62:72–83.
44. Needham SR, Roberts SK, Arkhipov A, et al. EGFR oligomerization organizes kinase-active dimers into competent signalling platforms. Nat Commun. 2016;7:13307.
45. Sarabipour S, Hristova K. Mechanism of FGF receptor dimerization and activation. Nat Commun. 2016;7:10262.
46. Purba ER, Saita E-I, Maruyama IN. Activation of the EGF receptor by ligand binding and oncogenic mutations: The "rotation model". Cells. 2017;6:13.
47. Petersen KJ, Peterson KC, Muretta JM, Higgins SE, Gillispie GD, Thomas DD. Fluorescence lifetime plate reader: Resolution and precision meet high-throughput. Rev Sci Instrum. 2014;85:113101.
48. Lo CH, Lim CK-W, Ding Z, et al. Targeting the ensemble of heterogeneous tau oligomers in cells: A novel small molecule screening platform for tauopathies. Alzheimers Dement. 2019;15:1489–1502.
49. Gruber SJ, Cornea RL, Li J, et al. Discovery of enzyme modulators via high-throughput time-resolved FRET in living cells. J Biomol Screen. 2014;19:215–222.
50. Dremencov E, Folgering JHA, Hogg S, Tecott L, Cremers TIFH. The role of 5-HT2C receptors in the pathophysiology and treatment of depression. In: di Giovanni G, Esposito E, di Matteo V, editors. 5-HT2C receptors in the pathophysiology of CNS disease. Totowa, NJ: Humana Press, 2011; p. 249–260.
51. Nau F Jr, Yu B, Martin D, Nichols CD. Serotonin 5-HT2A receptor activation blocks TNF-α mediated inflammation in vivo. PLoS One. 2013;8:e75426.
52. Yu B, Becnel J, Zerfaoui M, Rohatgi R, Boulares AH, Nichols CD. Serotonin 5-hydroxytryptamine$_{2A}$ receptor activation suppresses tumor necrosis factor-α-induced inflammation with extraordinary potency. J Pharmacol Exp Therap. 2008;327:316–323.
53. Pelletier M, Siegel RM. Wishing away inflammation? New links between serotonin and TNF signaling. Mol Interventions. 2009;9:299–301.
54. Knauer CS, Campbell JE, Chio CL, Fitzgerald LW. Pharmacological characterization of mitogen-activated protein kinase activation by recombinant human 5-HT2C, 5-HT2A, and 5-HT2B receptors. Naunyn Schmiedebergs Arch Pharmacol. 2009;379:461–471.
55. Herrick-Davis K, Grinde E, Harrigan TJ, Mazurkiewicz JE. Inhibition of serotonin 5-hydroxytryptamine2C receptor function through heterodimerization: Receptor dimers bind two molecules of ligand and one G-protein. J Biol Chem. 2005;280:40144–40151.
56. Bonaventure P, Nepomuceno D, Miller K, et al. Molecular and pharmacological characterization of serotonin 5-HT2A and 5-HT2B receptor subtypes in dog. Eur J Pharmacol. 2005;513:181–192.
57. Herrick-Davis K, Grinde E, Mazurkiewicz JE. Biochemical and biophysical characterization of serotonin 5-HT2C receptor homodimers on the plasma membrane of living cells. Biochemistry. 2004;43:13963–13971.
58. Kotecki M, Reddy PS, Cochran BH. Isolation and characterization of a near-haploid human cell line. Exp Cell Res. 1999;252:273–280.
59. Day ES, Cote SM, Whitty A. Binding efficiency of protein–protein complexes. Biochemistry. 2012;51:9124–9136.
60. Hayden MS, Ghosh S. Regulation of NF-κB by TNF family cytokines. Semin Immunol. 2014;26:253–266.
61. Andera L. Signaling activated by the death receptors of the TNFR family. Biomed Pap Med Fac Univ Palacky Olomouc Czech Repub. 2009;153:173–180.
62. Tortarolo M, Vallarola A, Lidonnici D, et al. Lack of TNF-alpha receptor type 2 protects motor neurons in a cellular model of amyotrophic lateral sclerosis and in mutant SOD1 mice but does not affect disease progression. J Neurochem. 2015;135:109–124.
63. Perez C, Albert I, DeFay K, Zachariades N, Gooding L, Kriegler M. A nonsecretable cell surface mutant of tumor necrosis factor (TNF) kills by cell-to-cell contact. Cell. 1990;63:251–258.
64. Sipe KJ, Dantzer R, Kelley KW, Weyhenmeyer JA. Expression of the 75 kDA TNF receptor and its role in contact-mediated neuronal cell death. Brain Res Mol Brain Res. 1998;62:111–121.
65. Zacharias DA, Violin JD, Newton AC, Tsien RY. Partitioning of lipid-modified monomeric GFPs into membrane microdomains of live cells. Science. 2002;296:913–916.
66. Zhang JH, Chung TD, Oldenburg KR. A simple statistical parameter for use in evaluation and validation of high throughput screening assays. J Biomol Screen. 1999;4:67–73.
67. Birmingham A, Selfors LM, Forster T, et al. Statistical methods for analysis of high-throughput RNA interference screens. Nat Methods. 2009;6:569–575.
68. Schaaf TM, Peterson KC, Grant BD, et al. High-throughput spectral and lifetime-based FRET screening in living cells to identify small-molecule effectors of SERCA. SLAS Discov. 2017;22:262–273.

SUPPORTING INFORMATION

Additional supporting information may be found online in the Supporting Information section at the end of this article.

How to cite this article: Lo CH, Huber EC, Sachs JN. Conformational states of TNFR1 as a molecular switch for receptor function. *Protein Science*. 2020;29:1401–1415. https://doi.org/10.1002/pro.3829